

of radiation-damage processes have been well documented: The details of the mathematical formalisms within which EPR results are generally analyzed can be found in several publications, e.g., Refs. 11 and 12.

¹¹G. Watkins, in *Effets Des Rayonnements Sur Les Semiconducteurs* (unpublished).

¹²G. Watkins, *IEEE Trans. NS-16*, No. 6 (1969).

¹³B. Goldstein, *Phys. Rev. Letters* **17**, 1 (1966).

¹⁴E. M. Pell, *Phys. Rev.* **119**, 1222 (1960).

¹⁵G. D. Watkins *et al.*, *J. Appl. Phys.* **30**, 1198 (1959).

¹⁶This step also removed the surface EPR states.

¹⁷This was "Wetalloy-232" obtained from the Victor King Laboratories.

¹⁸R. L. Aggarwall *et al.*, *Phys. Rev.* **138**, A882 (1965).

¹⁹G. D. Watkins, *Bull. Am. Phys. Soc.* **10**, 303 (1965).

²⁰G. D. Watkins and J. W. Corbett, *Phys. Rev.* **134**, A1359 (1964).

²¹J. Bourgoin *et al.*, in *Radiation Effects* (to be published).

²²The first report of such changes was made by Carter [*IEEE Trans. NS-14*, 110 (1967)] on float-zone material, although the report of spontaneous recovery of radiation-

damaged solar cells at room temperature, Ref. 9, should perhaps also be mentioned.

²³G. Feher, *Phys. Rev.* **114**, 1219 (1969).

²⁴I am indebted to G. Watkins for this information prior to publication.

²⁵The Fermi level here must be somewhere within $\lesssim kT$ (0.0023 eV) of the shallow donor energy.

²⁶G. Watkins, in *Radiation Damage in Semiconductors* (Dunod, Paris, 1965).

²⁷The over-all sensitivity of our instrumentation was such that we should have seen defect introduction rates as low as 10^{-4} cm^{-1} .

²⁸Hall measurements (of carrier concentration and mobility) have recently been made which indicate that both Li-defect formation and Li-defect dissociation can take place with time at room temperature in Li-doped electron-irradiated Si [G. Brucker (private communication)].

²⁹G. Watkins and J. Corbett, *Phys. Rev.* **138**, A543 (1965).

³⁰L. Cheng *et al.*, *Phys. Rev.* **152**, A761 (1966).

³¹R. E. Whan, *J. Appl. Phys.* **37**, 3378 (1966).

³²R. M. Chrenko *et al.*, *Phys. Rev.* **138**, A1775 (1965).

Properties of Spontaneous and Stimulated Emission in GaAs Junction Lasers. I. Densities of States in the Active Regions

C. J. Hwang

Bell Telephone Laboratories, Murray Hill, New Jersey 07974

(Received 27 March 1970)

The densities of states in the conduction and valence bands appropriate for the p region of the junction have been calculated self-consistently in the screened potential and effective-mass approximations. Such a density of states for one particular band consists of a tail part taken from the theory of Halperin and Lax, an unperturbed parabolic density of states above the tail, and a smooth interpolation in between. The use of the unperturbed parabolic band is justified, since the perturbation technique of Bonch-Bruевич and a straightforward second-order perturbation calculation both show that the distortion of the band due to the presence of impurities at the concentration employed in a typical laser is less than 5%. Contrary to the generally accepted assumption and Stern's calculation using Kane's density of states of a long and reasonable large conduction band tail, our results show that the tail is negligibly small compared to the valence band tail. On the basis of this calculation, it is concluded that, for a typical laser, the electron quasi-Fermi level at lasing threshold for temperature above 77°K should be in the parabolic portion of the band and not in the tail as is often assumed without justification. The approximations of using linear screening for the impurity potentials and the Gaussian statistics for the impurity distribution which are implied in the density-of-state functions of Kane and of Halperin and Lax are considered in detail.

I. INTRODUCTION

Calculation of the properties of a semiconductor laser usually starts by computing the spontaneous emission rate in the region where the recombination takes place. Many of the observed characteristics of a GaAs junction laser such as the temperature dependence of the threshold current,¹⁻⁶ the lasing wavelength shift as a function of injection current,⁷ the rate,⁸ and the band shape² of the spontaneous emission have been interpreted by different

models, using various expressions for the density of states involved in the optical transitions. These calculations have been made either with or without the momentum-conservation selection rule but all have assumed a constant matrix element for the radiative transitions. In the calculations with the selection rule preserved, parabolic densities of states have been used for both the conduction and valence bands to compute the recombination rate and the stimulated emission function either on the

p side of the junction¹ or within the space-charge region of the junction.³ In the no-selection-rule approximation, the development of this type of calculation has followed the progress in the theory of band structure of impure semiconductors. Initially the parabolic density of states was used^{2,4} and later the effect of band tails taken from Kane's theory⁹ was included. The calculations were performed for the cases where the electrons are thermally injected into the p region and recombination takes place in that region. It was found that a smaller current is required to maintain a given gain and that a closer agreement is obtained for the gain-current relationship when the band tails are incorporated in the calculation.⁵ The density of states is, therefore, the primary quantity to be determined and the calculated results on the properties of spontaneous and stimulated emission may very well be affected by the densities of states used.

The density of states obtained from Kane's theory can be expressed in terms of the carrier screening length when a screened potential is used to describe the Coulomb interaction of all the charged particles. Since the screening length also depends on the density of states, the Fermi level and the temperature, the problem of determining these quantities can be solved self-consistently. Stern⁵ used this method to determine the parameters associated with the state density function and hence the spontaneous emission rate as a function of injection current. We have performed a similar calculation but using a different expression for the state density function and a matrix element given by Dumke¹⁰ which takes into account the decrease in transition probability for electron states with high crystal momentum. Our density of states consists of a tail part taken from the theory of Halperin and Lax,¹¹ also in the form of a screened potential approximation, and an unperturbed parabolic part above the tail. The use of the unperturbed parabolic band is justified, since calculations using perturbation techniques show only a negligible distortion of the band above the tail because of the presence of impurities at typical concentrations.

The need for such a calculation is apparent from several considerations. First, the constant matrix element may overestimate the total recombination rates at higher temperature because of the increase in population in the high momentum states. Second, it has been shown that,¹² owing to the omission of the kinetic energy of localization in the Thomas-Fermi treatment, Kane's theory predicts a substantially larger total number of states in the tail than that predicted by the theory of Halperin and Lax. Third, the effects of acceptors on the conduction band tail and the donors on the valence band tail were not included in Kane's expression or in Stern's calculation. Since the formation of a band

tail results from the potential fluctuation of the randomly distributed impurities, both the donors and acceptors should affect either of the two tails. In the present work, this correlation effect is automatically incorporated when the theory of Halperin and Lax is used.

In this paper, we compute the densities of states to be used in the following paper for the calculation of spontaneous and stimulated spectral functions. We first construct the density-of-states function from the band theory of heavily doped crystals using the effective-mass approximation. The band shifts due to Coulomb and exchange interactions are thus taken into account in this formulation. The calculated results of the densities of states are then compared with those obtained from Kane's theory. It is found that, contrary to the generally accepted assumption¹³ and the results of Stern's calculation, the conduction band tail spreads much less into the gap than does the valence band tail. Consequently, the electron quasi-Fermi level near the threshold should not be located in the conduction band tail as is often assumed¹⁴ but should be in the parabolic portion of the band for a typical laser above 77 °K. Finally, we discuss the approximations of using the linear screening and Gaussian statistics which were made by Kane, and Halperin and Lax to obtain analytical expressions for the density of states functions.

II. DENSITY-OF-STATES FUNCTIONS

We consider a medium corresponding to the p layer of the junction containing both donors and acceptors in such concentrations that the donor and acceptor bands merge, respectively, with the conduction and valence bands.¹⁵ In addition to the presence of holes, electrons are injected into the region. If it is assumed that the electron and hole thermalization times are short compared with their respective lifetimes, we are dealing with a non-equilibrium situation associated with considerable concentrations of electrons and holes, respectively, in the conduction and valence bands. In the effective-mass approximation, we can write the Hamiltonian for the system as $H = H_e + H_h$, where

$$H_e = \sum_i \left(-\frac{\hbar^2 \nabla_i^2}{2m_c^*} \right) + \frac{1}{2} \sum_{i \neq j} \left(\frac{e^2}{\epsilon |\vec{r}_i - \vec{r}_j|} \right) - \sum_{i,l} \left(\frac{ze^2}{\epsilon |\vec{r}_i - \vec{R}_l|} \right) - \frac{1}{2} \sum_{i,k} \left(\frac{e^2}{\epsilon |\vec{r}_i - \vec{s}_k|} \right) + N' E_c^0, \quad (1)$$

with a similar expression for H_h .¹⁶ In Eq. (1), the \vec{r}_i 's and \vec{s}_k 's are the electron and hole coordinates, the \vec{R}_l 's are the positions of the donors and acceptors whose charge states are denoted by z , m_c^* is the conduction band effective mass, N' is the total number of electrons, and E_c^0 is the energy of the $\vec{k}=0$ state in the pure crystal. A many-electron

treatment by Wolff¹⁷ using a Hamiltonian similar to H_e shows that the system of all electrons in the conduction band can be approximated by single electrons moving in the field of the screened impurity potentials provided that the whole conduction band is shifted downward by an amount equal to the exchange energy E_c^e and that the effective mass m_c^* is slightly modified. If we neglect the small change in m_c^* , the one-electron Hamiltonian of the same system can be written as

$$H_1 = \hbar^2 \nabla^2 / 2m_c^* - E_c^e + E_c^0 + V(\vec{x}), \quad (2)$$

where \vec{x} is the single electron coordinate, and $V(\vec{x})$ is the screened potential of the randomly distributed impurities. Defining the average of $V(\vec{x})$ as E_c^c , such that the potential fluctuation about E_c^c is $V'(\vec{x}) = V(\vec{x}) - E_c^c$, we can then express H_1 as

$$H_1 = -\hbar^2 \nabla^2 / 2m_c^* - E_c^e + E_c^c + E_c^0 + V'(\vec{x}). \quad (3)$$

Thus, in the case of no fluctuation [$V'(\vec{x})=0$], the eigenstates of H_1 are plane waves, and the density of states is parabolic for energy E greater than $E_c^0 - E_c^e + E_c^c$ and vanishes completely for E below $E_c^0 - E_c^e + E_c^c$. In the real crystal because of the random nature of the impurity distribution, $V'(\vec{x})$ at some \vec{x} will not be equal to zero. When the $V'(\vec{x})$ in question is sufficiently large and attractive, we expect to find a bound state localized in these regions. The density of such states is called the tail state density ρ_c^t for $E < E_c^0 - E_c^e + E_c^c$. Thus, if we define the conduction band edge energy of the impure crystal E_c as

$$E_c = E_c^0 - \Delta E_c, \quad (4)$$

where $\Delta E_c = E_c^e - E_c^c$, the density of states in the conduction band $\rho_c(E)$ for all energies can be expressed as

$$\rho_c(E) = \rho_c^p(E) + \rho_c^t(E), \quad (5)$$

where $\rho_c^p(E)$ is the density of states for $E > E_c$. In computing ρ_c^p , we treat $V'(\vec{x})$ as a perturbation to the system since the electronic states for $E > E_c$ will not be greatly affected by the presence of the impurities. Thus, in the approximation that $V'(\vec{x})$ can be expressed as superposition of all screened potentials due to individual impurities (linear screening), a second-order perturbation calculation yields an expression for $\rho_c^p(E)$ ¹²:

$$\begin{aligned} \rho_c^p(E) = \frac{1}{2\pi^2} \left(\frac{m_c^*}{\hbar^2} \right)^{3/2} \{ & (E - E_c - \frac{1}{4} E_{Qc}) \\ & + [(E - E_c + \frac{1}{4} E_{Qc})^2 + \xi]^{1/2} \}^{1/2} \{ 1 + [(E - E_c \\ & + \frac{1}{4} E_{Qc})^2 + \xi]^{-1/2} (E - E_c + \frac{1}{4} E_{Qc}) \}, \quad (6) \end{aligned}$$

where $E_{Qc} = \hbar^2 Q^2 / 2m_c^*$, $\xi = 2\pi e^4 (N_A + N_D) / Q\epsilon^2$ is the mean square of the impurity potential, m_c^* is the electron effective mass, Q is the reciprocal screen-

ing length, and N_A and N_D are, respectively, the acceptor and donor concentrations. It can be seen from Eq. (6) that $\rho_c^p(E)$ will depend on the impurity concentration and the injection level since both affect the value of Q . As an example, we plot in Fig. 1 as dashed curves the $\rho_c^p(E)$ and $\rho_v^p(E)$ for a case of $N_A = 6 \times 10^{18} \text{ cm}^{-3}$, $N_D = 3 \times 10^{18} \text{ cm}^{-3}$, $E_{Qc} = 0.124 \text{ eV}$, and $E_{Qv} = 0.0178 \text{ eV}$ (for simplicity, we have set $E_c = 0$ and $E_v = 0$ in plotting the curves). These numbers correspond to approximately the threshold condition at 300 °K for a typical laser with a total loss of 100 cm^{-1} .¹⁸ Also plotted for comparison is the parabolic density of states defined by

$$\rho_c^0(E) = (1/2\pi^2) (2m_c^* / \hbar^2)^{3/2} (E - E_c)^{1/2}. \quad (7)$$

It is seen that the deviation between $\rho_c^p(E)$ and $\rho_c^0(E)$ for all $E - E_c > 0$ is less than 5% in this particular case. The same small distortion is also true for the valence band. As the doping increases, the distortion is bigger, but is less than 10% for a laser with substrate doping of $N_D = 1 \times 10^{19} \text{ cm}^{-3}$, the heaviest doped crystal ever used for making reason-

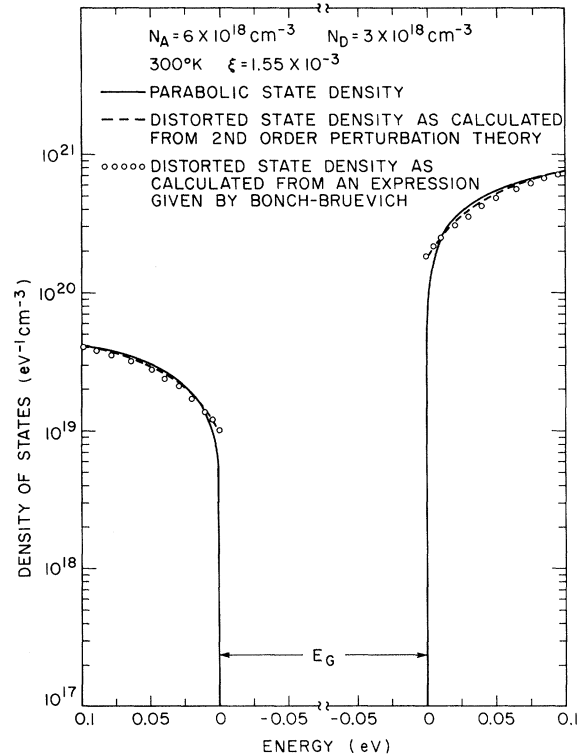


FIG. 1. Unperturbed and perturbed parabolic densities of state in the conduction and valence band. The perturbed curves are calculated from Eqs. (6) and (8) using $N_A = 6 \times 10^{18} \text{ cm}^{-3}$, $N_D = 3 \times 10^{18} \text{ cm}^{-3}$, $\xi = 1.55 \times 10^{-3} \text{ eV}^2$, $E_{Qc} = 0.124 \text{ eV}$, and $E_{Qv} = 0.0178 \text{ eV}$ which corresponds approximately the threshold condition at 300 °K for a typical laser with a total loss of 100 cm^{-1} .

ably good lasers. Hence, we shall set $\rho^p(E) = \rho^0(E)$ and shall call the density of states above the band edge as the parabolic density of states in this calculation.

It is interesting to note that Eq. (6) yields a result close to an expression given by Bonch-Bruevich,¹⁹

$$\rho_c^p(E) = \rho_c^0(E) \left[\frac{1}{4} (2\pi)^{1/2} \right] x^{1/2} e^{-x} \times [I_{1/4}(x) + I_{-1/4}(x) + I_{3/4}(x) + I_{-3/4}(x)], \quad (8)$$

where $x = E^2/4\xi$, and I 's are the Bessel functions with imaginary argument. Equation (8) is also plotted, as open circles, in Fig. 1. Since Eq. (8) is obtained from a more elaborate combination of perturbation and Green's-function techniques, one suspects that other perturbation methods such as Wolff's technique¹⁷ might also give similar small distortion of the parabolic band. We therefore feel justified in using the approximation $\rho_c^p(E) = \rho_c^0(E)$.

Using the Hamiltonian given by Eq. (3), Halperin and Lax obtained $\rho_c^t(E)$ by counting the number of local minima in some particular bound-state energy calculated variationally using a fixed wave function. In the case where linear screening for the impurity atoms and the Gaussian statistics for the impurity distribution can be approximated, $\rho_c^t(E)$ can be expressed as¹¹

$$\rho_c^t(E) = [(QE_{Qc})^3 / \xi^2] a(\mu_c) e^{-E_{Qc}^2 b(\mu_c)/2\xi}, \quad (9)$$

where $a(\mu_c)$ and $b(\mu_c)$ are functions of the dimensionless parameter $\mu_c = (E_c - E)/E_{Qc}$ and are tabulated in Ref. 11.

There will be a region just below $E = E_c$ in which Eq. (9) is not valid because of some of the approximations involved in deriving Eq. (9). We obtain the density of states in this region by a smooth but rather arbitrary interpolation. This is achieved by drawing, on a semilog plot, a straight line which will be made tangent to $\rho_c^0(E)$ at one end and $\rho_c^t(E)$ at the other. As we shall see, since the total number of states for $E < E_c$ is small compared to the total number of electrons for most cases, this uncertainty in the density of states is not expected to alter greatly our results.

Kane used the same Hamiltonian of Eq. (3) (also with the assumptions of linear screening and Gaussian statistics) but from the Thomas-Fermi approach to obtain the density of states in the form⁹

$$\rho_c^t(E') = \pi^{-2} \hbar^{-3} (m_c^*)^{3/2} (2\eta_c)^{1/2} y(E'/\eta_c), \quad (10)$$

where $\eta_c = (e^2/\epsilon) (4\pi N_D Q^{-1})^{1/2}$

and

$$y(x) = \pi^{-1/2} \int_{-\infty}^x (x-z)^{1/2} e^{-z^2} dz.$$

Only the donors are thus seen to affect the conduction band. Furthermore, the Thomas-Fermi treatment neglects the kinetic energy of localiza-

tion which is properly included in the theory of Halperin and Lax through the variational calculation. We shall see that as a result of this omission, Kane's theory predicts a substantially larger tail density of states than does the theory of Halperin and Lax.

III. BAND-GAP SHRINKAGE

In the past, the band gap of a pure crystal was often used in the calculation of spontaneous and stimulated emission spectra.²⁻⁶ Although the calculated results, except for the peak positions, will not be so much affected by the exact value of the energy gap, it is worth pointing out that because of Coulomb and exchange interactions the band-gap energy will no longer be equal to that of the pure crystal. We shall attempt to estimate the change in energy gap in this section.

From Eq. (4), we see that the effect of Coulomb and exchange interactions is to shift the whole conduction band by $\Delta E_c = E_c^e - E_c^c$. Such an interaction will also cause a shift of the valence band due to correlation effects. We shall, however, ignore this shift of the valence band in our calculation as did Bonch-Bruevich and Rozman²⁰ in their attempt to account for the absorption edge shift in heavily doped crystals and Ashin and Rogachev²¹ in their interpretation of the electroluminescence data.

Assuming that the same treatment can be applied to the free holes in the valence band, we find that the valence band edge E_v is shifted from the pure case E_v^0 by an amount $\Delta E_v = E_v^e + E_v^c$ and that $E_v = E_v^0 + \Delta E_v$. The energy gap E_g of the impure crystal can then be expressed as

$$E_g = (E_c^0 - \Delta E_c) - (E_v^0 + \Delta E_v) = E_g^0 - (\Delta E_c + \Delta E_v), \quad (11)$$

where $E_g^0 = E_c^0 - E_v^0$ is the energy gap of the pure crystal.

The band shift owing to exchange effects, E_c^e , can be estimated from a well-known expression by Wigner and Seitz in their calculation of cohesive energy in metals.²² It can be expressed in terms of the carrier concentration as^{18, 19, 23}

$$E_c^e = (4/b\pi\gamma_{sc}) (m_c^* e^4 / 2\epsilon^2 \hbar^2), \quad (12)$$

where $b = (4/9\pi)^{1/3}$ and γ_{sc} is the ratio of the average electron spacing $(3/4\pi N)^{1/3}$ to the effective Bohr radius $a_0 = \hbar^2 \epsilon / (m_c^* e^2)$ for electrons of concentration N in the conduction band. E_c^e is thus a function of the electron concentration. Equation (12) holds when $\gamma_{sc} < 1$. In most of our cases, the condition that $\gamma_{sc} < 1$ is satisfied for electrons but $\gamma_{sc} < 1$ is not well satisfied for holes in the valence band. Consequently, there will be some uncertainty in the calculated E_v^e . The band shift due to Coulomb interaction, E_c^c or E_v^c , is such that both E_c^c and E_v^c will

have the same sign. For a screened Coulomb potential and at very large carrier concentrations such that $\gamma_{sc} < 1$ and $\gamma_{sv} < 1$, we have¹¹

$$E_c^c = E_v^c = (4\pi e^2 / \epsilon Q^2) (N_A - N_D). \quad (13)$$

Again, since $\lambda_{sv} < 1$ is not quite satisfied, E_c^c may deviate from E_v^c . In this calculation, we shall assume $E_c^c = E_v^c$.

Because of the assumptions used to treat the band edge shifts, there will inevitably be some uncertainty in the calculation of E_g . This will mainly affect the positions of the spontaneous and absorption spectra but will not appreciably affect the calculated absorption constant as will be discussed in paper II. From a comparison of the peak positions of the experimental and calculated spontaneous spectra, also to be found in paper II, we find that the estimated band gap described in this section agrees with experiment to better than 1%.

IV. COMPUTER CALCULATIONS OF THE DENSITY OF STATES

The reciprocal screening constant Q under the assumption of linear screening can be expressed as²⁴

$$Q^2 = \frac{4\pi e^2}{\epsilon} \left[\int_v \rho_v(E) \frac{-\partial f_v(E)}{\partial E} dE + \int_c \rho_c(E) \frac{-\partial f_c(E)}{\partial E} dE \right], \quad (14)$$

where f_v and f_c are, respectively, the Fermi functions for holes in the valence band and electrons in the conduction bands. Since both $\rho_v(E)$ and $\rho_c(E)$ depend on Q , it can be seen from Eq. (14) that the problem of determining Q and other parameters such as the carrier concentrations can be solved self-consistently for a given value of the electron quasi-Fermi level E_{fe} . The steps have been described by Stern.⁵ Briefly, we regard the donor and acceptor concentrations as the primary input parameters. The net hole concentration P is determined from the charge neutrality conditions $P - N = N_A - N_D$. The value of E_{fe} , which gives the degree of injection, is the variable for each set of N_A and N_D at a specified temperature. For a given E_{fe} and a given temperature, a trial value of Q is assumed. Since ρ_c and ρ_v are then known, the electron and hole concentrations and the hole quasi-Fermi level E_{fh} can be found from an iteration procedure.¹² The input E_{fe} and the value of E_{fh} thus determined are substituted in Eq. (14) and a new Q is determined. If the new Q is different from the trial Q , it is then used as the trial Q and the process is continued. The calculation for Q will stop when the difference between the final Q and the preceding Q is equal to 1% of the preceding Q value. The uncertainty involved in the

calculation is 0.5 meV for E_{fe} and E_{fh} , and is $2 \times 10^{15} \text{ cm}^{-3}$ for N and P . The integration grid is 0.5 meV in the iteration process. From this calculation, we can determine self-consistently the values of Q , E_{fh} , N , P altogether at the same time for a given degree of injection represented by E_{fe} . The calculation was performed with the aid of a CDC-6600 computer. The following constants appropriate for GaAs were used: $m_c^* = 0.072 m_0$, $m_v^* = 0.5 m_0$, and $\epsilon = 12.5$, where m_0 is the free-electron mass.

V. RESULTS

The density-of-states functions $\rho_c(E)$ given by Eq. (5) and $\rho_c'(E)$ given by Eq. (10) which are calculated self-consistently for an n -type GaAs crystal doped with $N_D = 6 \times 10^{18} \text{ cm}^{-3}$ are plotted in Fig. 2. The extent of the difference between Kane's theory and the theory of Halperin and Lax can be clearly seen. Kane's theory predicts a substantially larger total number of states in the tail than that predicted by the theory of Halperin and Lax, i. e., $\rho_c(E)$ decreases more rapidly and spreads much less into the energy gap. In Fig. 3, we compare the shapes of $\rho_c(E)$ and $\rho_c'(E)$ for $N_A = 6 \times 10^{18} \text{ cm}^{-3}$ and $N_D = 3 \times 10^{18} \text{ cm}^{-3}$ at an injection level equal to the threshold of a typical laser with a total loss of

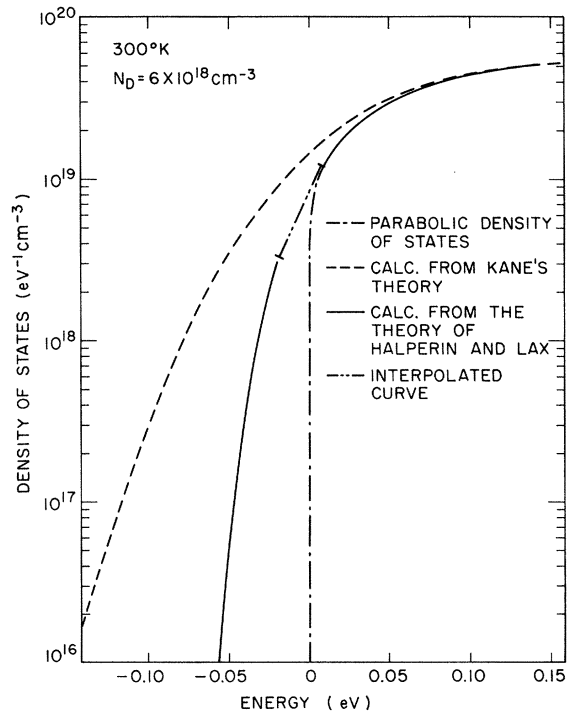


FIG. 2. Conduction-band densities of states at 300°K as calculated self-consistently from parabolic, Kane's, and Halperin and Lax's expressions using donor concentration of $N_D = 6 \times 10^{18} \text{ cm}^{-3}$.

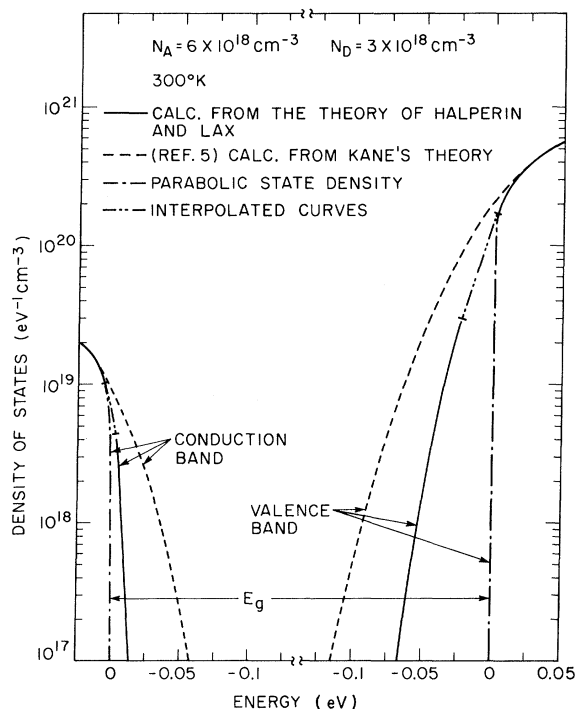


FIG. 3. Comparison of the structures of the self-consistent densities of states at 300 °K obtained from different models for $N_A = 6 \times 10^{18} \text{ cm}^{-3}$ and $N_D = 3 \times 10^{18} \text{ cm}^{-3}$. The injection level for this calculation is approximately equal to the threshold condition at 300 °K for a typical laser with a total loss of 100 cm^{-1} .

100 cm^{-1} at 300 °K. The big difference in the structure of the band tails is again seen for the compensated crystal. The most striking feature of our results is that the conduction band tail is negligibly small compared with the valence band tail at all injection levels. Physically, such a distribution of the densities of states can be easily understood from a comparison of carrier screening length with the effective Bohr radii for electrons and holes. At all injection levels below the threshold of a typical laser, the screening length ($\sim 20 \text{ \AA}$) is much smaller than the Bohr radius for electrons (92 \AA), but is greater than the Bohr radius for holes (13.3 \AA). Thus, the potential fluctuation which results in the formation of the tails will be practically screened out for electrons but not for holes. Our calculation appears to support a model proposed earlier by Bagaev *et al.*²⁵ from the uncertainty principle argument that it is possible to have a negligible conduction band tail in the active region for a substrate doping greater than $1 \times 10^{18} \text{ cm}^{-3}$.

Figure 4 shows the temperature variation of the electron and hole quasi-Fermi levels at the lasing threshold for lasers with a total loss of $\alpha_L = 100$ and 120 cm^{-1} ; and $N_A = 6 \times 10^{18} \text{ cm}^{-3}$ and $N_D = 3 \times 10^{18}$

cm^{-3} in the active region. The results with band tails (given by Kane's theory) and without band tails are also shown for comparison. The Fermi levels are referred, respectively, to the conduction and valence band edges, and they are positive when measured into the corresponding band. Two important features should be noted. First, the functional variation of Fermi levels with temperature is nearly the same for all models. This will have some effect on the temperature dependence of the current required to reach a certain gain as will be seen in paper II. Secondly, our calculation shows that the electron quasi-Fermi level should be located in the parabolic portion of the conduction band and not in the tail portion. Although Stern's calculation using Kane's model for the band tails predicts that the electron quasi-Fermi level should be in the tail below 300 °K in the same case, it is merely due to the overestimation of the total number of states in the tail as was pointed out previously.²⁶ A calculation for the cases with $N_D = 3 \times 10^{18} \text{ cm}^{-3}$

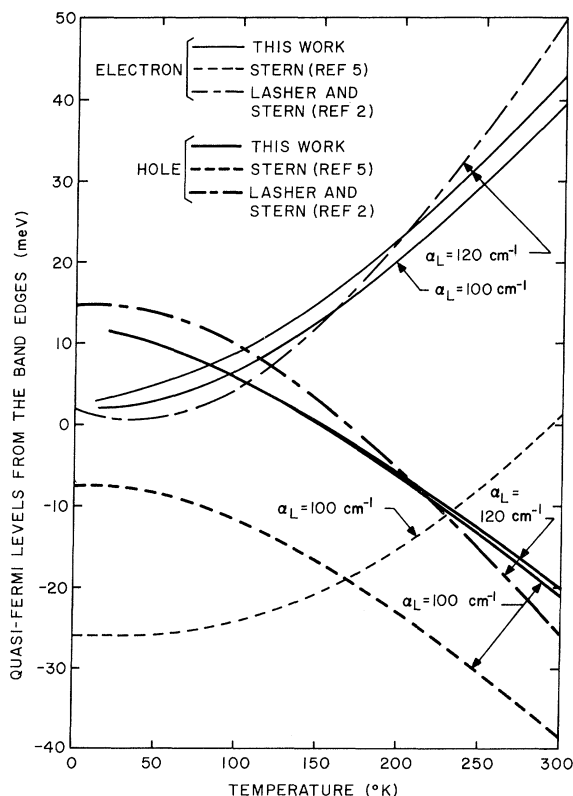


FIG. 4. Temperature dependences of electron and hole quasi-Fermi levels calculated for $N_A - N_D (= 3 \times 10^{18} \text{ cm}^{-3}) = 3 \times 10^{18} \text{ cm}^{-3}$ but using different expressions for the density of states. The injection level for this calculation is approximately equal to the threshold conditions at 300 °K for two typical lasers with losses of 100 and 120 cm^{-1} , respectively.

and an N_A value ranging from 4×10^{18} to $8 \times 10^{18} \text{ cm}^{-3}$ shows that the electron quasi-Fermi levels at the lasing threshold for temperatures above $77 \text{ }^\circ\text{K}$ should not be in the tail for lasers with total loss greater than 50 cm^{-1} .

The results of this section would appear to throw some doubt on the validity of earlier work on GaAs junction lasers. It has been almost invariably assumed, with no justification, that the conduction band tail is long and large enough to contain the electron quasi-Fermi level. The analysis of the experimental data and the theoretical calculation of the properties of a laser have started from this presumption. There are usually several arbitrary constants to adjust so that it has usually been possible to account for the experimental data by varying these constants. Take, for example, the good fit between the experimental and calculated electroluminescence spectra at low temperatures using an exponential conduction-band density of states.² Since the electroluminescence at low temperature and at low bias has now been shown to be due to radiative tunneling from the n side by electrons and the p side by holes into the space charge region,²⁷ the good agreement must be fortuitous and simply associated with the arbitrary adjustment of the three parameters (the electron quasi-Fermi level, the preexponential density of states and the band tailing constant). Our calculations here show that it is risky to assume that (i) the electron quasi-Fermi level is in the conduction band tail in predicting laser behavior²⁸ or (ii) to explain the observed properties of a laser^{13,14,29} as was frequently done in the past.

VI. DISCUSSION OF THE CALCULATION

All the assumptions involved in the calculation were discussed in Secs. II-IV. Here we turn to the two most basic assumptions used to obtain the expressions for the density of states, Eq. (9) or Eq. (10), in the treatments of Kane, and Halperin and Lax, i. e., (i) the validity of using linear screening for each individual impurity potential and (ii) Gaussian statistics for the random impurity distribution. The assumptions should be good when the concentrations of carriers and impurities are sufficiently high. However, it is hard to determine in either case a precise minimum concentration below which any one of these assumptions ceases to apply. On the other hand, one could give an injection level above which each assumption is certain to be valid. The reason for using the injection level as a parameter is that, for a laser, the total impurity concentration is fixed and the carrier screening can only be changed at a fixed temperature by changing the injected electron concentration. We shall use the case in which $N_A = 6 \times 10^{18} \text{ cm}^{-3}$ and $N_D = 3 \times 10^{18} \text{ cm}^{-3}$ as an example. However, our

result in this section should be almost true for any lasers made from Zn diffusion from a Ga-Zn alloy source into a substrate doped with $N_D = 3 \times 10^{18} \text{ cm}^{-3}$.

For linear screening to be valid, the root-mean-square fluctuation in the total impurity potential $\xi^{1/2}$ should be small compared with the electron or or hole quasi-Fermi levels¹¹:

$$\xi^{1/2} < E_{fe} - E_c, \quad (15)$$

or

$$\xi^{1/2} < -(E_{fh} - E_v). \quad (16)$$

In Fig. 5, we plot the injection levels above which Eqs. (15) and (16) are satisfied as a function of temperature. Linearization in screened potentials for electrons should be strictly valid in the region above curve 1 and for holes above curve 3. Also plotted in the same figure are the values of the electron and hole quasi-Fermi levels required to obtain a gain of 100 cm^{-1} . It is seen that linear screening is really not strictly applicable in a laser with loss equal to 100 cm^{-1} for electrons and holes except for electrons near $300 \text{ }^\circ\text{K}$. The reason for this difficulty is that the total impurity concentration

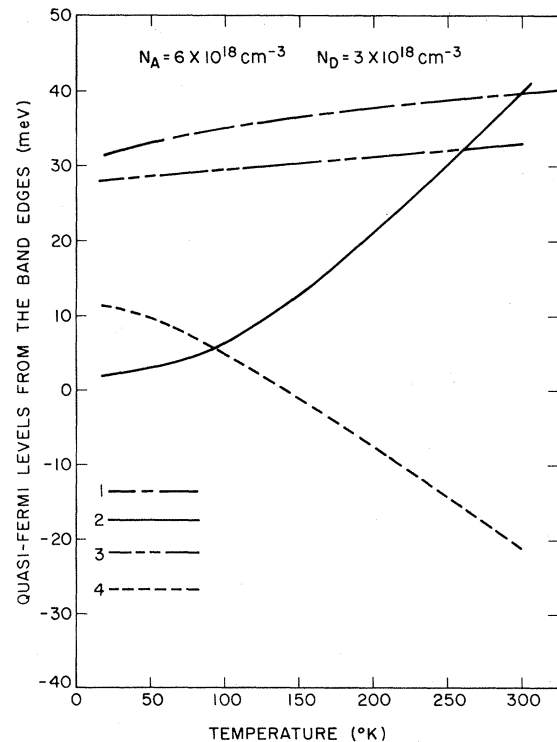


FIG. 5. Curves 1 and 3: Minimum injection levels above which linearization of the individual screened potentials for electrons and holes is strictly valid for a laser with $N_A = 6 \times 10^{18} \text{ cm}^{-3}$ and $N_D = 3 \times 10^{18} \text{ cm}^{-3}$ in the active region. Curves 2 and 4: The values of the electron and hole quasi-Fermi levels required to obtain a gain of 100 cm^{-1} .

is always greater than the sum of the electron and hole concentrations. It is not clear how the validity of the linear screening will be affected by the failure of satisfying Eqs. (15) and (16). Reasonably good quantitative agreement with experiment, to be described in paper II, indicates that the approximation might not be too bad.

Halperin and Lax¹¹ give an expression for the minimum electron and hole energies below which the density of states in the tail calculated by using the Gaussian statistics for the impurity distribution should not be assured to be valid:

$$-(E - E_c) < E_{Qe} [(N_A + N_D) Q^{-3}]^{2/3} / \{1 - [(N_A + N_D) Q^{-3}]^{1/3}\}, \quad (17)$$

for electrons and

$$E - E_v < E_{Qv} [N_A + N_D] Q^{-3}]^{2/3} / \{1 - [(N_A + N_D) Q^{-3}]^{1/3}\}, \quad (18)$$

for holes. In Fig. 6, we plot (curves 1 and 3) the right-hand side of Eqs. (17) and (18), respectively, for 20, 77, and 300 °K, as functions of an injection level. The energy region to the right of each curve gives the energy range in which the density of states can strictly be calculated using Gaussian statistics. We also plot (curves 2 and 4) the respective electron and hole energies at which the density of states is equal to 0.1% ($\sim 10^{16} \text{ cm}^{-3} \text{ eV}^{-1}$) of the density of states at the conduction band edge and 1% of the density of states at the valence band edge. It is seen that at all injection levels, Gaussian statistics can be used to calculate practically the whole energy range of the conduction band tail, since the density of states in the tail decreases rapidly below $10^{16} \text{ cm}^{-3} \text{ eV}^{-1}$. This is not true for the valence band tail even above the energy value corresponding to 1% of the density of states at the band edge. This difficulty is due to the fact that in all cases, while the carrier screening length is small compared to the Bohr radius for electrons, it is still large compared to the Bohr radius for holes, and that the condition for the high-concentration limit is that the screening length should be small compared to the Bohr radius. Again, even though we are not certain about the range of validity of the approximation resulting from using Gaussian statistics to compute the valence band tail state density, we have assumed that Gaussian statistics can be used in our calculation. The good agreement of the calculated spontaneous emission band shape in the superradiance region with experiment, to be described in paper II, should support this assumption.

One important conclusion can be drawn from a calculation of the conduction band density of states at 300 °K. At 300 °K, the linear screening and Gaussian statistics are both valid for electrons and there should be little uncertainty in the calculated structure of the conduction band tail. It is therefore safe to state that for a typical diffused diode with $\alpha_L > 100 \text{ cm}^{-1}$ at 300 °K the conduction band at an injection level corresponding to the threshold is negligibly small and that the electron quasi-Fermi level should be far up in the parabolic portion of the band.

ACKNOWLEDGMENTS

I wish to thank R. L. Brown for computer programming. I am also indebted to Dr. F. Stern, Dr. E. O. Kane, and Dr. R. A. Faulkner for valuable comments, and to Dr. E. C. Lightowers for a critical reading of the manuscript.

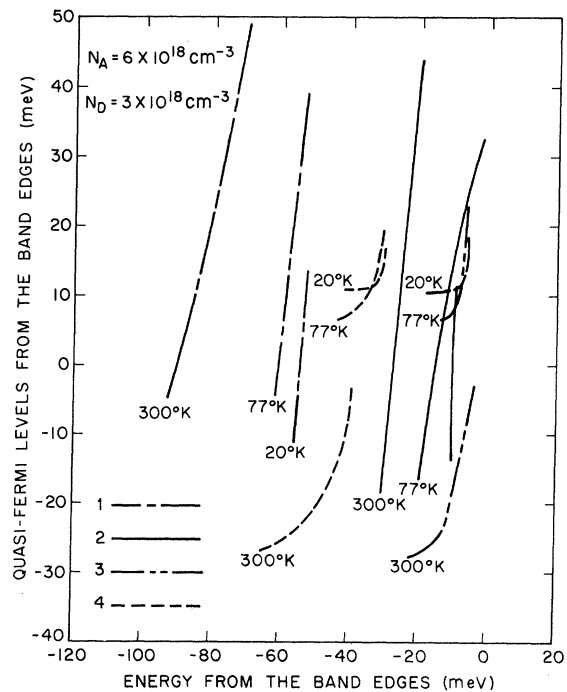


FIG. 6. Energy range in which Gaussian statistics can strictly be used to calculate the densities of states in the conduction and valence band tails for a laser with $N_A = 6 \times 10^{18} \text{ cm}^{-3}$ and $N_D = 3 \times 10^{18} \text{ cm}^{-3}$ in the active region. Curve 1: Energy above which the Gaussian statistics for the impurity distribution is strictly valid for electrons. Curve 2: Energy at which the conduction band density of states is equal to 0.1% of that at the parabolic band edge. Curve 3: Energy below which Gaussian statistics for the impurity distribution is strictly valid for holes. Curve 4: Energy at which the valence band density of states is equal to 1% of that at the parabolic band edge.

- ¹R. N. Hall, *Solid-State Electron.* 6, 405 (1963).
- ²G. Lasher and F. Stern, *Phys. Rev.* 133, A553 (1964).
- ³G. E. Pikus, *Fiz. Tverd. Tela* 7, 3536 (1965) [*Soviet Phys. Solid State* 7, 2854 (1966)].
- ⁴K. Unger, *Z. Physik* 207, 322 (1967).
- ⁵F. Stern, *Phys. Rev.* 148, 186 (1966).
- ⁶K. Unger, *Z. Physik* 207, 332 (1967).
- ⁷H. Yonezu, A. Kawaji, and Y. Yasuoka, *Solid-State Electron.* 11, 129 (1968).
- ⁸H. Sato, *Japan. J. Appl. Phys.* 7, 409 (1967).
- ⁹E. O. Kane, *Phys. Rev.* 131, 79 (1963).
- ¹⁰W. P. Dumke, *Phys. Rev.* 132, 1998 (1963).
- ¹¹B. I. Halperin and M. Lax, *Phys. Rev.* 148, 722 (1966).
- ¹²C. J. Hwang, *J. Appl. Phys.* 41, 2668 (1970).
- ¹³See, for example, M. H. Pilkuhn, *Phys. Status Solidi* 25, 9 (1968).
- ¹⁴See, for example, G. C. Dousmanis and D. L. Staebler, *J. Appl. Phys.* 37, 2278 (1966).
- ¹⁵This corresponds to a donor concentration of greater than $6 \times 10^{16} \text{ cm}^{-3}$ { see O. V. Emel'yarenko *et al.*, *Fiz. Tverd. Tela* 7, 1315 (1965) [*Soviet Phys. Solid State*, 7, 1063 (1965)] } and an acceptor concentration of greater than $4 \times 10^{18} \text{ cm}^{-3}$ [see, for example, F. Ermanis and K. B. Wolfstirn, *J. Appl. Phys.* 37, 1963 (1966)].
- ¹⁶In what follows, we shall use the conduction band as an example. The valence band can easily be obtained by substituting appropriate parameters. We shall denote the parameters associated with the conduction band by the subscript *c* and those associated with the valence band by the subscript *v*.
- ¹⁷P. A. Wolff, *Phys. Rev.* 126, 405 (1962).
- ¹⁸The laser threshold is defined as the injection level required to maintain a gain which is equal to the total loss of the laser. The gain is defined in turn as the maximum of the negative absorption coefficient to be described in paper II.
- ¹⁹See, for example, V. L. Bonch-Bruevick, in *Physics of III-V Compounds*, edited by R. K. Willardson and A. C. Beer (Academic, New York, 1966), Vol. I, p. 101.
- ²⁰V. L. Bonch-Bruevich and R. Rozman, *Fiz. Tverd. Tela* 6, 2535 (1964) [*Soviet Phys. Solid State*, 6, 2016 (1965)].
- ²¹V. M. Asnin and A. A. Rogachev, *Fiz. Tverd. Tela* 5, 1730 (1963) [*Soviet Phys. Solid State* 5, 1257 (1963)].
- ²²N. F. Mott and H. Jones, *The Theory of Properties of Metals and Alloys* (Dover, New York, 1936), p. 137.
- ²³M. Gell-Mann and A. K. Brueckner, *Phys. Rev.* 106, 364 (1957).
- ²⁴See, for example R. B. Dingle, *Phil. Mag.* 46, 831 (1955).
- ²⁵V. S. Bagaev, Yu. N. Berozashvili, B. M. Vul, E. I. Zavaritskaya, L. V. Keldysh, and A. P. Shotov, *Fiz. Tverd. Tela* 6, 1399 (1964) [*Soviet Phys. Solid State* 6, 1093 (1964)]; in *Proceedings of the International Conference of Semiconductors. 4. Radiative Recombination in Semiconductors, Paris, 1964* (Dunod, Paris, 1964), p. 149.
- ²⁶In this connection, the electron quasi-Fermi level calculated by Unger (Ref. 6) using an exponential density of states in the tail should also be located in the tail since the total number of tail states was normalized to that predicted by Kane's model.
- ²⁷H. C. Casey, Jr., and D. J. Silversmith, *J. Appl. Phys.* 40, 241 (1969).
- ²⁸See, for example, A. N. Chakravarti, *Intern. J. Electron.* 23, 375 (1968); M. J. Adams, *Solid-State Electron.* 12, 661 (1969).
- ²⁹G. J. Burrell, T. S. Moss, and A. Hetherington, *Solid-State Electron.* 12, 787 (1969).